Crystal structure and Hirshfeld surface analysis of the elusive trichlorobis(diethyl ether)oxo-molybdenum(V)

Thomas E. Shaw,[a,b] Pierre LeMagueres,[c] Alfred P. Sattelberger[a]* and Titel Jurca[a,b]*

[a]Department of Chemistry, University of Central Florida, Orlando, FL 32816, USA, [b]Renewable Energy and Chemical Transformations Cluster, University of Central Florida, Orlando, FL 32816, USA, and [c]Rigaku Americas Corporation, The Woodlands, TX 77381, USA. *Correspondence e-mail: al.sattelberger@knights.ucf.edu, titel.jurca@ucf.edu

First reported in 1930, $MoCl_3O(Et_2O)_2$ is a by-product of the reductive synthesis of $MoCl_4(OEt_2)_2$ from $MoCl_5$. We report herein the X-ray crystal structure and Hirshfeld surface characteristics of *mer*-$MoCl_3O(Et_2O)_2$, or $[MoCl_3O(C_4H_{10}O)_2]$. The compound crystallizes in the orthorhombic space group $P2_12_12_1$. The molybdenyl (Mo=O) bond length is 1.694 (3) Å and the *cis*- and *trans*-Mo—O distances are 2.157 (3) and 2.304 (3) Å, respectively. Intermolecular Mo=O···H bonding is present in the lattice, with the shortest distance being 2.572 Å.

1. Introduction

The red–orange diethyl ether adduct of molybdenum(IV) chloride, $MoCl_4(OEt_2)_2$ (**1**), is a useful synthon for mid-valent molybdenum chemistry (Kuiper *et al.*, 2008a,b). It can be prepared anaerobically by reducing a suspension of molybdenum pentachloride, $MoCl_5$, in diethyl ether with any one of the following reductants: norbornene (Castellani & Gallazzi, 1985), allyltrimethylsilane (Persson & Andersson, 1993), or elemental tin (Stoffelbach *et al.*, 2001). **1** is sparingly soluble in ether and easily isolated by filtration. The crystalline solid slowly loses ether on standing at room temperature and more rapidly under vacuum. Each of the published preparations provide **1** in ≥80% yield. Two of the reported syntheses (Castellani & Gallazzi, 1985; Stoffelbach *et al.*, 2001) note that if either the diethyl ether is not sufficiently dry and/or the $MoCl_5$ is contaminated with oxyhalides, the green molybdenum(V) oxo–chloro compound $MoCl_3O(OEt_2)_2$ (**2**) forms as a by-product. The latter compound was first reported in 1930 (Wardlaw & Webb, 1930). The solid-state structure of **2** (Scheme 1) has never been reported and is the subject of the present work.

Scheme 1
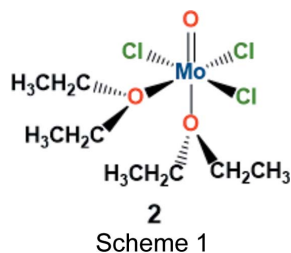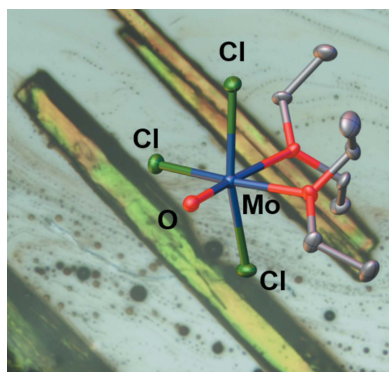
2. Experimental

2.1. Synthesis and crystallization

Compound **1** was prepared essentially as described by Persson & Andersson (1993), by adding excess $C_3H_5SiMe_3$ dropwise to a stirred diethyl ether suspension of $MoCl_5$ inside

Table 1
Experimental details.

Crystal data	
Chemical formula	$[MoCl_3O(C_4H_{10}O)_2]$
M_r	366.53
Crystal system, space group	Orthorhombic, $P2_12_12_1$
Temperature (K)	100
a, b, c (Å)	8.6186 (7), 12.250 (1), 13.5681 (11)
V (Å^3)	1432.5 (2)
Z	4
Radiation type	Mo $K\alpha$
μ (mm^{-1})	1.46
Crystal size (mm)	$0.6 \times 0.21 \times 0.16$
Data collection	
Diffractometer	Rigaku XtaLAB Mini II
Absorption correction	Gaussian (*CrysAlis PRO*; Rigaku Oxford Diffraction, 2020)
T_{min}, T_{max}	0.614, 0.831
No. of measured, independent and observed [$I > 2\sigma(I)$] reflections	7488, 3179, 2959
R_{int}	0.042
$(\sin\theta/\lambda)_{max}$ (Å^{-1})	0.649
Refinement	
$R[F^2 > 2\sigma(F^2)]$, $wR(F^2)$, S	0.033, 0.069, 1.01
No. of reflections	3179
No. of parameters	153
H-atom treatment	H atoms treated by a mixture of independent and constrained refinement
$\Delta\rho_{max}$, $\Delta\rho_{min}$ (e Å^{-3})	0.53, −0.87
Absolute structure	Flack x determined using 1123 quotients $[(I^+) − (I^-)]/[(I^+) + (I^-)]$ (Parsons et al., 2013)
Absolute structure parameter	0.01 (5)

Computer programs: *CrysAlis PRO* (Rigaku Oxford Diffraction, 2020), *SHELXT2018* (Sheldrick, 2015a), *SHELXL2018* (Sheldrick, 2015b) and *OLEX2* (Dolomanov et al., 2009).

an mBraun inert atmosphere glove-box (water and O_2 levels of ≤1 ppm). For practical reasons, the reaction was carried out at approximately −30 °C rather than at the reported −78 °C. The red–orange solid product, which formed immediately at

low temperature upon addition of the silane, was stirred for 2 h at room temperature and then filtered off and washed with fresh diethyl ether collected on an mBraun solvent purification system. The red–orange filtrate was concentrated to *ca* 15 ml, placed in a scintillation vial, and stored in the −35 °C freezer of the glove-box. After several days, a well-formed dark-green crystal of **2** was observed at the bottom of the vial. A crystal of **2** with dimensions $0.16 \times 0.21 \times 0.60$ mm was removed from the mother liquor, coated with Paratone oil, removed from the glove-box, quickly secured to a MiteGen micromount, and mounted on the diffractometer under a cryostream (100 K) to prevent the loss of diethyl ether. Notably, **2** rapidly degrades in Paratone under ambient conditions (Fig. S1 in the supporting information).

2.2. Refinement

Crystal data, data collection and structure refinement details are summarized in Table 1. H atoms were attached *via* the riding model at calculated positions.

3. Results and discussion

$MoCl_3O(Et_2O)_2$ (**2**) crystallized in the enantiomorphic space group $P2_12_12_1$ with a single molecule in the asymmetric unit. The structure and atom-labeling scheme are shown in Fig. 1(*a*). A partially occupied unit cell, with hydrogen bonding represented by dashed lines, is shown in Fig. 1(*b*). Expanded packing diagrams of eight unit cells ($2 \times 2 \times 2$) are displayed in the supporting information (Fig. S2); beyond the description of hydrogen-bonding interactions provided (*vide infra*), there are no remarkable features requiring further discussion. The isolated $MoCl_3O(Et_2O)_2$ complex exists in a distorted octahedral geometry, with the chloro ligands adopting a meridional configuration. This is consistent with predicted structures and analogous oxomolybdenum complexes with
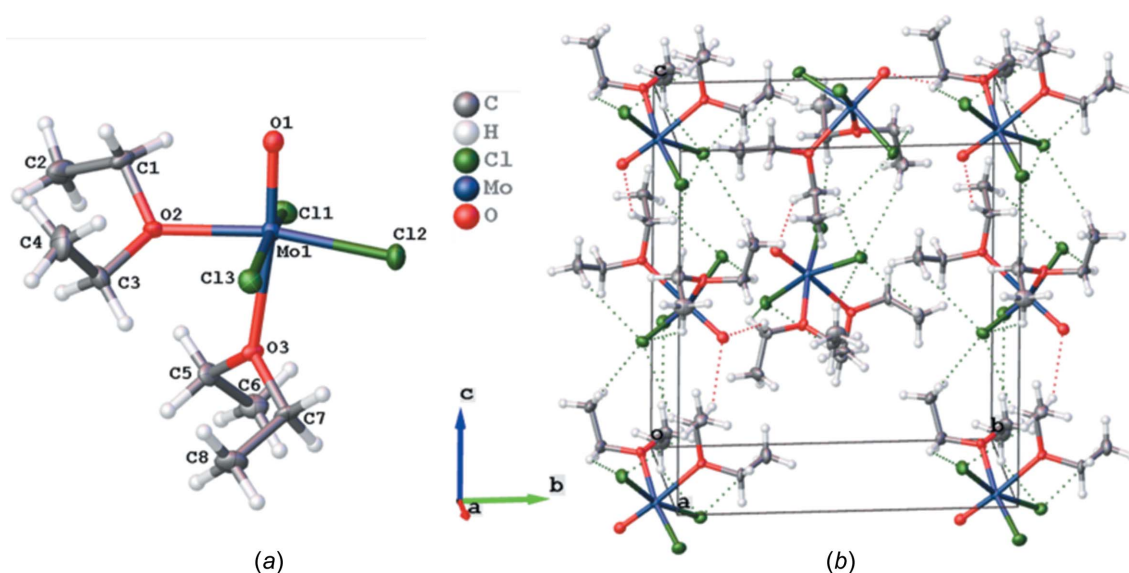
Figure 1
(*a*) The asymmetric unit of **2**, showing the labeling scheme for the complex. Displacement ellipsoids are drawn at the 50% probability level. (*b*) The partially filled $P2_12_12_1$ unit cell of **2**, showing the inter- and intramolecular hydrogen-bonding interactions.
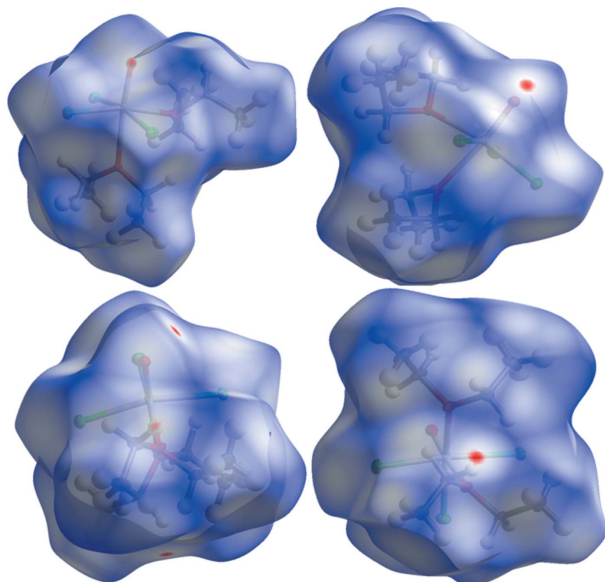
Figure 2
d_{norm} Hirshfeld surface of MoCl$_3$O(Et$_2$O)$_2$ from various viewpoints highlighting the areas of intimate contact.

Table 2
Selected geometric parameters (Å, °).

Mo1—Cl1	2.3469 (13)	Mo1—O3	2.304 (3)
Mo1—Cl3	2.3530 (13)	O2—C1	1.468 (6)
Mo1—Cl2	2.3159 (13)	O2—C3	1.463 (6)
Mo1—O1	1.694 (3)	O3—C5	1.455 (5)
Mo1—O2	2.157 (3)	O3—C7	1.463 (5)
O1—Mo1—O3	173.06 (14)	O1—Mo1—O2	93.09 (14)
O2—Mo1—Cl2	168.30 (9)	O3—Mo1—Cl2	88.37 (9)
Cl1—Mo1—Cl3	165.00 (5)	O3—Mo1—Cl1	82.92 (8)
O1—Mo1—Cl2	98.48 (12)	O3—Mo1—Cl3	82.19 (8)
O1—Mo1—Cl1	98.02 (11)	O2—Mo1—O3	80.10 (11)
O1—Mo1—Cl3	96.55 (11)		

solvent ligands coordinated through the O heteroatoms (Castellani & Gallazzi, 1985; Stoffelbach *et al.*, 2001; Vitzthumecker *et al.*, 2017; Marchetti *et al.*, 2013). Selected bond lengths are shown in Table 2, showcasing the metal-to-ligand bond lengths and angles.

As expected, the O atom of the diethyl ether ligand that is *trans* to the molybdenum–oxo bond is elongated [2.304 (3) Å] compared to the O atom *trans* to a meridional chloro ligand [2.157 (3) Å]. In fact, the molybdenum–oxo bond length, as well as the lengths of the meridional chloro ligands, are similar to analogous complexes (Table 3) (Marchetti *et al.*, 2013; Vitzthumecker *et al.*, 2017; Di Nicola *et al.*, 2015). The slight differences in the bond lengths of the meridional chloro ligands can be explained by the donating nature of the coordinating solvents. The only complex with longer Mo—O(solvent) bonds is MoCl$_3$O(H$_3$COCH$_2$CH$_2$OCH$_2$Cl), which is likely a result of the chloro functioning as a weak electron-withdrawing group. The lability of the diethyl ether ligands and the relatively short lifetime of the isolated MoCl$_3$O-(Et$_2$O)$_2$ complex under ambient conditions can thus be explained by the elongated Mo—O(solvent) bonds (Fig. S1 in the supporting information).
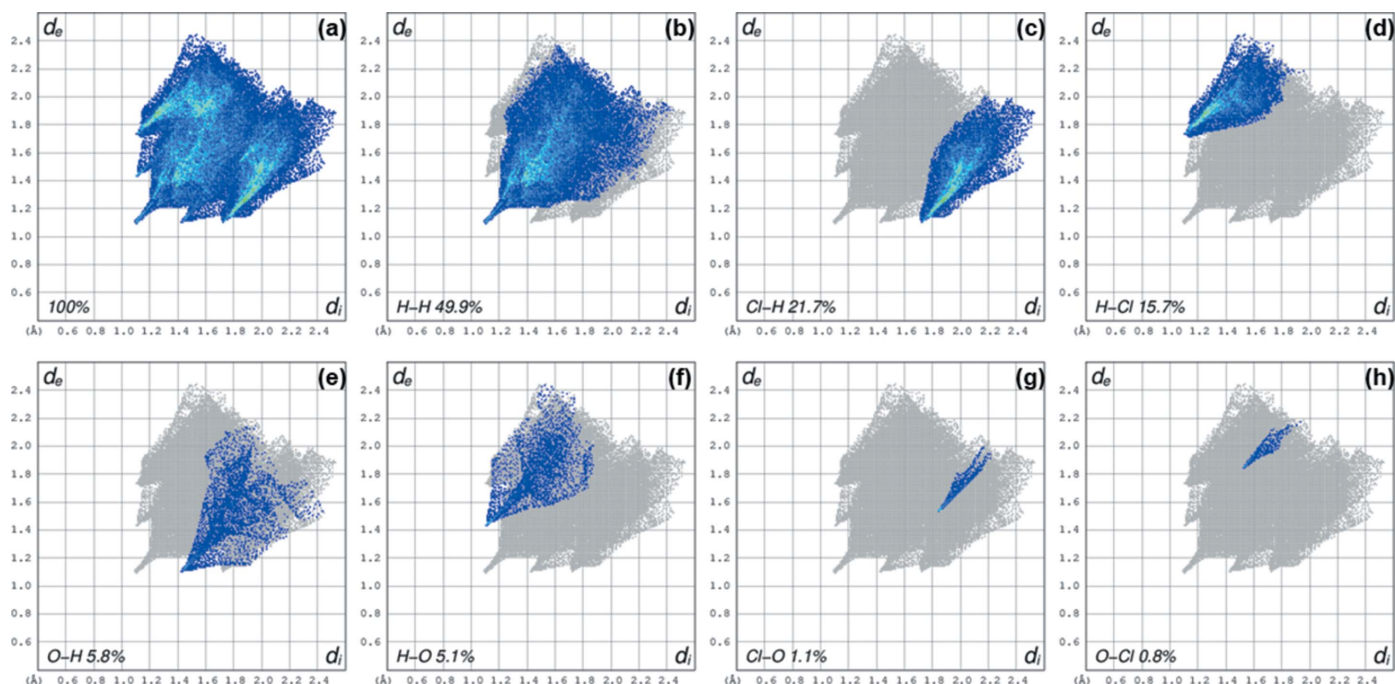
Figure 3
Two-dimensional (2D) fingerprint plots identifying the percent composition of the Hirshfeld surface from the various noncovalent interactions, with the accompanying percent contribution to the Hirshfeld surface: (*a*) the complete fingerprint plot accounting for all interactions, (*b*) interactions between interior and exterior H atoms, (*c*) interactions between interior Cl and exterior H atoms, (*d*) interactions between interior H and exterior Cl atoms, (*e*) interactions between interior O and exterior H atoms, (*f*) interactions between interior H and exterior O atoms, (*g*) interactions between interior Cl and exterior O atoms, and (*h*) interactions between interior O and exterior Cl atoms.

Table 3
Comparative Mo—*L* and Mo—*X* bond lengths of MoCl₃O(Et₂O)₂ (**2**) and analogous complexes.

The ligand represented by 'thf' is tetrahydrofuran.

MoCl₃O(Et₂O)₂	MoCl₃O(thf)₂ (Marchetti *et al.*, 2013)	MoCl₃O(MeOH)₂ (Vitzthumecker *et al.*, 2017)	MoCl₃[MeO(CH₂)₂OCH₂Cl] (Di Nicola *et al.*, 2015)
Mo1—Cl1 2.3469 (13)	Mo—Cl2 2.3513 (9)	Mo1—Cl2 2.3642 (8)	Mo1—Cl5 2.3542 (8)
Mo1—Cl3 2.3530 (13)	Mo—Cl1 2.3646 (8)	Mo1—Cl1 2.3434 (7)	Mo1—Cl4 2.3453 (7)
Mo1—Cl2 2.3159 (13)	Mo—Cl3 2.3191 (9)	Mo1—Cl3 2.3741 (9)	Mo1—Cl2 2.3216 (7)
Mo1—O2 2.157 (3)	Mo—O2(thf) 2.146 (2)	Mo—O2 2.099 (2)	Mo1—O2 2.161 (2)
Mo1—O3 2.304 (3)	Mo—O3(thf) 2.277 (2)	Mo—O3 2.266 (2)	Mo1—O3 2.420 (2)
Mo1—O1 1.694 (3)	Mo—O1(oxo) 1.682 (2)	Mo—O1 1.655 (2)	Mo1—O1 1.666 (2)

There are instances of intermolecular hydrogen bonding that occur between the molybdenum–oxo linkage and neighboring diethyl ether ligands. Specifically, Mo1＝O1···H1*B*ⁱ—C1ⁱ and Mo1＝O1···H5*B*ⁱⁱ—C5ⁱⁱ [symmetry codes: (i) $x - \frac{1}{2}, -y + \frac{1}{2}, -z + 1$; (ii) $-x + \frac{1}{2}, -y + 1, z + \frac{1}{2}$], with bond lengths of 2.683 and 2.572 Å, respectively (Fig. 1*b*). These two bonding interactions explain the extended Mo1＝O1 bond distance [1.694 (3) Å] compared to analogous oxomolybdenum complexes (Table 3). An intramolecular close contact is also present between two meridional chloro ligands and neighboring diethyl ether H atoms, *viz.* Cl1···H1*A*—C1, Cl3···H4*B*—C4, and Cl3···H8*B*—C8, with bond lengths of 2.697, 2.949, and 2.946 Å, respectively. Atom Cl3 also experiences an intermolecular contact through Cl3···H5*A*ⁱⁱ—C5ⁱⁱ and Cl3···H2*A*ⁱⁱ—C2ⁱⁱ, with bond lengths of 2.926 and 2.927 Å, respectively. These close contacts are a direct cause of the extended Mo—Cl bond lengths of Mo1—Cl1 and Mo1—Cl3 (Table 2). A basal plane was generated through the meridional plane of the complex with the equation $-0.272x + 0.709y - 0.650z - 0.536 = 0$ (Fig. S3 in the supporting information). The distance of the molybdenum centre from the centroid of the basal plane is 0.264 Å and the fractional coordinates from the atom projection to the plane are (0.134701, 0.460936, 0.478813). This centre–centroid distance is shorter than that reported for the MoCl₃O(MeOH)₂ and MoCl₃O[MeO(CH₂)₂OCH₂Cl] adducts, which display respective distances of 0.322 and 0.378 Å, but is similar to that of MoCl₃O(PMe₃)(O＝PMe₃), which has a distance of 0.256 Å (Marchetti *et al.*, 2013; Limberg *et al.*, 1996).

The d_{norm} Hirshfeld surface (−0.0313 to 1.2958 Å) was generated using *CrystalExplorer17* (Turner *et al.*, 2017) and can be seen in Fig. 2. There are four red portions of the surface, generated by interactions that are shorter than van der Waals radii, all of which are the result of Mo＝O···H—C interactions between the CH₂ hydrogens of the coordinated diethyl ether and the Mo＝O oxygen. Two of these interactions are the result of exterior diethyl ether hydrogens near the interior Mo＝O bond, while the other two are caused by two exterior Mo＝O bonds interacting with interior diethyl ether ligands. The Hirshfeld surface with neighboring atoms and molecules is elaborated in Fig. S4 (see supporting information). The spatial configuration of neighboring molecules is a direct result of these close contact interactions, causing the coordinated diethyl ethers to lie in proximity to one another. Because of this, the majority of the Hirshfeld surface is the result of H···H interactions between interior and exterior diethyl ethers, which account for 49.9% of the surface (Fig. 3*b*). The points of intimate contact between the diethyl ether H atoms and the molybdenum–oxo bonds account for a total of 10.9% of the surface (Figs. 3*d* and 3*e*). Intriguingly, contact between the meridional chloro ligands and diethyl ether H atoms account for 37.4% of the Hirshfeld surface, but do not account for any of the close contact points of the surface. The remaining percentages of the Hirshfeld surface can be seen in the remainder of Fig. 3. As expected, no portions of the surface are caused by interactions, both interior and exterior, from Mo or C atoms.

4. Conclusion

The crystal structure and Hirshfeld surface character of *mer*-MoCl₃O(Et₂O)₂, along with fingerprint-plot analysis, have been reported. The chloro ligands adopt a meridional configuration, with one diethyl ether ligand coordinated *trans* to a chloro ligand and one *trans* to the molybdenum–oxo bond. The molybdenum–diethyl ether bond *trans* to the molybdenum–oxo bond is noticeably longer than seen in analogous complexes, consistent with the lability of the coordinated diethyl ether. Intermolecular hydrogen bonds occur between the molybdenum–oxo bond and the CH₂ diethyl ether groups of neighboring complexes. Unresolved is the source of the molybdenyl O atom in **2**. All reagents were of high purity and the liquid starting materials were thoroughly dried and deoxygenated. The yield of **2** described above was estimated to be <5%. When a second reaction was carried out with identical quantities of the same reagents, but closer to room temperature, the filtrate was green and the yield of **2** increased significantly (>10%). We surmise from this result that diethyl ether is at least a contributing source of the molybdenyl O atom in **2**. Further work would be needed to identify the organic side products and develop a mechanistic picture of exactly how the oxygen transfer occurs. With a confirmed structure, the door is open for implementation of *mer*-MoCl₃O(Et₂O)₂ (**2**) as a potential oxomolybdenum(V) synthon.

References

Castellani, L. & Gallazzi, M. C. (1985). *Transition Met. Chem.* **10**, 194–195.

Di Nicola, F. P., Lanzi, M., Marchetti, F., Pampaloni, G. & Zacchini, S. (2015). *Dalton Trans.* **44**, 12653–12659.

Dolomanov, O. V., Bourhis, L. J., Gildea, R. J., Howard, J. A. K. & Puschmann, H. (2009). *J. Appl. Cryst.* **42**, 339–341.

Kuiper, D. S., Douthwaite, R. E., Mayol, A.-R., Wolczanski, P. T., Lobkovsky, E. B., Cundari, T. R., Lam, O. P. & Meyer, K. (2008a). *Inorg. Chem.* **47**, 7139–7153.

Kuiper, D. S., Wolczanski, P. T., Lobkovsky, E. B. & Cundari, T. R. (2008b). *Inorg. Chem.* **47**, 10542–10553.

Limberg, C., Büchner, M., Heinze, K. & Walter, O. (1996). *Inorg. Chem.* **36**, 872–879.

Marchetti, F., Pampaloni, G. & Zacchini, S. (2013). *Dalton Trans.* **42**, 15226–15234.

Parsons, S., Flack, H. D. & Wagner, T. (2013). *Acta Cryst.* B**69**, 249–259.

Persson, C. & Andersson, C. (1993). *Inorg. Chim. Acta*, **203**, 235–238.

Rigaku Oxford Diffraction (2020). *CrysAlis PRO*. Rigaku Oxford Diffraction, Yarnton, Oxfordshire, England.

Sheldrick, G. M. (2015a). *Acta Cryst.* A**71**, 3–8.

Sheldrick, G. M. (2015b). *Acta Cryst.* C**71**, 3–8.

Stoffelbach, F., Saurenz, D. & Poli, R. (2001). *Eur. J. Inorg. Chem.* **2001**, 2699–2703.

Turner, M. J., McKinnon, J. J., Wolff, S. K., Grimwood, J. D., Spackman, P. R., Jayatilaka, D. & Spackman, M. A. (2017). *CrystalExplorer17*. University of Western Australia. https://hirsh-feldsurface.net.

Vitzthumecker, C., Robinson, F. & Pfitzner, A. (2017). *Monatsh. Chem.* **148**, 629–633.

Wardlaw, W. & Webb, H. W. (1930). *J. Chem. Soc.* pp. 2100–2106.

Crystal structure and Hirshfeld surface analysis of the elusive trichlorobis(diethyl ether)oxomolybdenum(V)

Thomas E. Shaw, Pierre LeMagueres, Alfred P. Sattelberger and Titel Jurca

Computing details

Data collection: *CrysAlis PRO* (Rigaku Oxford Diffraction, 2020); cell refinement: *CrysAlis PRO* (Rigaku Oxford Diffraction, 2020); data reduction: *CrysAlis PRO* (Rigaku Oxford Diffraction, 2020); program(s) used to solve structure: SHELXT2018 (Sheldrick, 2015a); program(s) used to refine structure: *SHELXL2018* (Sheldrick, 2015b); molecular graphics: OLEX2 (Dolomanov *et al.*, 2009); software used to prepare material for publication: OLEX2 (Dolomanov *et al.*, 2009).

Trichloridobis(diethyl ether)oxidomolybdenum(V)

Crystal data

$[MoCl_3O(C_4H_{10}O)_2]$	$D_x = 1.700$ Mg m^{-3}
$M_r = 366.53$	Mo $K\alpha$ radiation, $\lambda = 0.71073$ Å
Orthorhombic, $P2_12_12_1$	Cell parameters from 3727 reflections
$a = 8.6186$ (7) Å	$\theta = 2.2$–$30.5°$
$b = 12.250$ (1) Å	$\mu = 1.46$ mm^{-1}
$c = 13.5681$ (11) Å	$T = 100$ K
$V = 1432.5$ (2) Å^3	Block, green
$Z = 4$	$0.6 \times 0.21 \times 0.16$ mm
$F(000) = 740$	

Data collection

Rigaku XtaLAB Mini II diffractometer	3179 independent reflections
	2959 reflections with $I > 2\sigma(I)$
Absorption correction: gaussian (CrysAlis PRO; Rigaku Oxford Diffraction, 2020)	$R_{int} = 0.042$
	$\theta_{max} = 27.5°$, $\theta_{min} = 2.2°$
	$h = -11 \rightarrow 10$
$T_{min} = 0.614$, $T_{max} = 0.831$	$k = -15 \rightarrow 15$
7488 measured reflections	$l = -17 \rightarrow 16$

Refinement

Refinement on F^2	$w = 1/[\sigma^2(F_o^2) + (0.0278P)^2]$
Least-squares matrix: full	where $P = (F_o^2 + 2F_c^2)/3$
$R[F^2 > 2\sigma(F^2)] = 0.033$	$(\Delta/\sigma)_{max} < 0.001$
$wR(F^2) = 0.069$	$\Delta\rho_{max} = 0.53$ e Å^{-3}
$S = 1.01$	$\Delta\rho_{min} = -0.87$ e Å^{-3}
3179 reflections	Extinction correction: SHELXL2018
153 parameters	(Sheldrick, 2015b),
0 restraints	Fc*=kFc[1+0.001xFc$^2\lambda^3$/sin(2θ)]$^{-1/4}$
Hydrogen site location: mixed	Extinction coefficient: 0.0042 (6)
H atoms treated by a mixture of independent and constrained refinement	

Absolute structure: Flack *x* determined using
1123 quotients [(I+)-(I-)]/[(I+)+(I-)] (Parsons et
al., 2013)
Absolute structure parameter: 0.01 (5)

Special details

Geometry. All esds (except the esd in the dihedral angle between two l.s. planes) are estimated using the full covariance matrix. The cell esds are taken into account individually in the estimation of esds in distances, angles and torsion angles; correlations between esds in cell parameters are only used when they are defined by crystal symmetry. An approximate (isotropic) treatment of cell esds is used for estimating esds involving l.s. planes.

Fractional atomic coordinates and isotropic or equivalent isotropic displacement parameters (Å^2)

	x	*y*	*z*	U_{iso}*/U_{eq}
Mo1	0.14299 (5)	0.44571 (3)	0.49142 (3)	0.01453 (13)
Cl3	0.28566 (14)	0.58992 (10)	0.56149 (9)	0.0189 (3)
Cl1	−0.00756 (16)	0.33468 (10)	0.38785 (9)	0.0220 (3)
Cl2	−0.07724 (14)	0.49900 (10)	0.57657 (9)	0.0209 (3)
O2	0.3298 (4)	0.4174 (3)	0.3888 (2)	0.0174 (8)
O3	0.0863 (4)	0.5768 (2)	0.3751 (2)	0.0144 (7)
O1	0.2054 (4)	0.3474 (3)	0.5698 (2)	0.0168 (8)
C5	0.0851 (6)	0.5576 (4)	0.2693 (3)	0.0182 (11)
H5A	0.135 (6)	0.491 (4)	0.258 (4)	0.022*
H5B	0.160 (6)	0.612 (4)	0.235 (4)	0.022*
C6	−0.0733 (6)	0.5618 (4)	0.2246 (4)	0.0236 (12)
H6A	−0.066049	0.547134	0.153769	0.035*
H6B	−0.118133	0.634422	0.235048	0.035*
H6C	−0.139516	0.506695	0.255753	0.035*
C7	0.0422 (6)	0.6881 (4)	0.4026 (4)	0.0190 (12)
H7A	0.027585	0.691699	0.474858	0.023*
H7B	−0.058213	0.706262	0.371106	0.023*
C3	0.4417 (6)	0.4994 (4)	0.3559 (4)	0.0224 (12)
H3A	0.396033	0.572873	0.364903	0.027*
H3B	0.461479	0.489161	0.284577	0.027*
C1	0.3840 (7)	0.3043 (5)	0.3786 (4)	0.0229 (13)
H1A	0.289 (6)	0.265 (4)	0.396 (4)	0.027*
H1B	0.467 (6)	0.293 (4)	0.421 (4)	0.027*
C8	0.1614 (7)	0.7714 (4)	0.3723 (4)	0.0286 (13)
H8A	0.174268	0.769715	0.300548	0.043*
H8B	0.260723	0.754567	0.404031	0.043*
H8C	0.126930	0.844267	0.392619	0.043*
C2	0.4275 (8)	0.2761 (4)	0.2751 (4)	0.0314 (14)
H2A	0.340121	0.291847	0.231139	0.047*
H2B	0.453518	0.198366	0.271139	0.047*
H2C	0.517573	0.319693	0.255101	0.047*
C4	0.5935 (6)	0.4942 (5)	0.4102 (4)	0.0346 (15)
H4A	0.647842	0.426657	0.392671	0.052*
H4B	0.573964	0.495383	0.481324	0.052*
H4C	0.657549	0.557115	0.391958	0.052*

Atomic displacement parameters (Å²)

	U^{11}	U^{22}	U^{33}	U^{12}	U^{13}	U^{23}
Mo1	0.01522 (19)	0.0139 (2)	0.0144 (2)	−0.00072 (17)	0.00121 (18)	−0.00088 (18)
Cl3	0.0200 (6)	0.0202 (6)	0.0165 (6)	−0.0034 (5)	−0.0024 (5)	−0.0025 (5)
Cl1	0.0286 (7)	0.0161 (6)	0.0213 (7)	−0.0050 (6)	−0.0044 (6)	−0.0019 (6)
Cl2	0.0174 (6)	0.0251 (7)	0.0202 (7)	0.0015 (6)	0.0047 (6)	−0.0008 (6)
O2	0.0203 (18)	0.0119 (17)	0.0200 (18)	0.0030 (14)	0.0045 (15)	0.0044 (14)
O3	0.0205 (17)	0.0124 (18)	0.0103 (16)	0.0035 (14)	−0.0016 (14)	−0.0012 (14)
O1	0.0164 (17)	0.0174 (18)	0.0166 (18)	0.0003 (15)	0.0010 (15)	−0.0014 (16)
C5	0.025 (3)	0.021 (3)	0.009 (2)	0.002 (3)	0.002 (2)	−0.002 (2)
C6	0.029 (3)	0.023 (3)	0.019 (3)	0.000 (3)	−0.007 (2)	−0.001 (3)
C7	0.024 (3)	0.008 (2)	0.024 (3)	0.004 (2)	−0.001 (2)	−0.001 (2)
C3	0.022 (3)	0.023 (3)	0.022 (3)	−0.004 (2)	0.007 (2)	0.003 (2)
C1	0.031 (3)	0.018 (3)	0.020 (3)	0.012 (2)	0.002 (3)	0.002 (2)
C8	0.041 (3)	0.014 (3)	0.031 (3)	−0.001 (3)	−0.003 (3)	0.000 (2)
C2	0.051 (4)	0.021 (3)	0.022 (3)	0.011 (3)	0.007 (3)	−0.003 (3)
C4	0.019 (3)	0.050 (4)	0.035 (3)	−0.001 (3)	0.005 (3)	−0.001 (3)

Geometric parameters (Å, º)

Mo1—Cl1	2.3469 (13)	C7—H7B	0.9900
Mo1—Cl3	2.3530 (13)	C7—C8	1.506 (7)
Mo1—Cl2	2.3159 (13)	C3—H3A	0.9900
Mo1—O1	1.694 (3)	C3—H3B	0.9900
Mo1—O2	2.157 (3)	C3—C4	1.502 (7)
Mo1—O3	2.304 (3)	C1—H1A	0.97 (5)
O2—C1	1.468 (6)	C1—H1B	0.93 (5)
O2—C3	1.463 (6)	C1—C2	1.493 (7)
O3—C5	1.455 (5)	C8—H8A	0.9800
O3—C7	1.463 (5)	C8—H8B	0.9800
C5—H5A	0.93 (5)	C8—H8C	0.9800
C5—H5B	1.04 (5)	C2—H2A	0.9800
C5—C6	1.494 (7)	C2—H2B	0.9800
C6—H6A	0.9800	C2—H2C	0.9800
C6—H6B	0.9800	C4—H4A	0.9800
C6—H6C	0.9800	C4—H4B	0.9800
C7—H7A	0.9900	C4—H4C	0.9800
O1—Mo1—O3	173.06 (14)	O3—C7—C8	112.6 (4)
O2—Mo1—Cl2	168.30 (9)	H7A—C7—H7B	107.8
Cl1—Mo1—Cl3	165.00 (5)	C8—C7—H7A	109.1
O1—Mo1—Cl2	98.48 (12)	C8—C7—H7B	109.1
O1—Mo1—Cl1	98.02 (11)	O2—C3—H3A	108.9
O1—Mo1—Cl3	96.55 (11)	O2—C3—H3B	108.9
O1—Mo1—O2	93.09 (14)	O2—C3—C4	113.3 (4)
O3—Mo1—Cl2	88.37 (9)	H3A—C3—H3B	107.7
O3—Mo1—Cl1	82.92 (8)	C4—C3—H3A	108.9

O3—Mo1—Cl3	82.19 (8)	C4—C3—H3B	108.9
O2—Mo1—O3	80.10 (11)	O2—C1—H1A	100 (3)
Cl2—Mo1—Cl3	90.87 (5)	O2—C1—H1B	109 (3)
Cl2—Mo1—Cl1	90.51 (5)	O2—C1—C2	112.7 (4)
O2—Mo1—Cl3	89.52 (9)	H1A—C1—H1B	115 (4)
O2—Mo1—Cl1	86.14 (10)	C2—C1—H1A	109 (3)
C3—O2—Mo1	125.4 (3)	C2—C1—H1B	110 (3)
C3—O2—C1	114.2 (4)	C7—C8—H8A	109.5
C1—O2—Mo1	116.8 (3)	C7—C8—H8B	109.5
C5—O3—Mo1	124.4 (3)	C7—C8—H8C	109.5
C5—O3—C7	113.6 (4)	H8A—C8—H8B	109.5
C7—O3—Mo1	122.0 (3)	H8A—C8—H8C	109.5
O3—C5—H5A	107 (3)	H8B—C8—H8C	109.5
O3—C5—H5B	110 (3)	C1—C2—H2A	109.5
O3—C5—C6	113.7 (4)	C1—C2—H2B	109.5
H5A—C5—H5B	101 (4)	C1—C2—H2C	109.5
C6—C5—H5A	113 (3)	H2A—C2—H2B	109.5
C6—C5—H5B	111 (3)	H2A—C2—H2C	109.5
C5—C6—H6A	109.5	H2B—C2—H2C	109.5
C5—C6—H6B	109.5	C3—C4—H4A	109.5
C5—C6—H6C	109.5	C3—C4—H4B	109.5
H6A—C6—H6B	109.5	C3—C4—H4C	109.5
H6A—C6—H6C	109.5	H4A—C4—H4B	109.5
H6B—C6—H6C	109.5	H4A—C4—H4C	109.5
O3—C7—H7A	109.1	H4B—C4—H4C	109.5
O3—C7—H7B	109.1		
Mo1—O2—C3—C4	98.5 (5)	C5—O3—C7—C8	−68.7 (5)
Mo1—O2—C1—C2	143.0 (4)	C7—O3—C5—C6	−67.0 (5)
Mo1—O3—C5—C6	110.8 (4)	C3—O2—C1—C2	−57.5 (6)
Mo1—O3—C7—C8	113.4 (4)	C1—O2—C3—C4	−58.9 (6)